

# Endogenous Proteolytic Cleavage of Normal and Disease-Associated Isoforms of the Human Prion Protein in Neural and Non-Neural Tissues

Adolfo Jiménez-Huete,\* Patricia M. J. Lievens,<sup>†</sup>  
Rubén Vidal,\* Pedro Piccardo,<sup>‡</sup>  
Bernardino Ghetti,<sup>‡</sup> Fabrizio Tagliavini,<sup>†</sup>  
Blas Frangione,\* and Frances Prelli\*

From the Department of Pathology,\* New York University Medical Center, New York, New York; the Istituto Nazionale Neurologico Carlo Besta,<sup>‡</sup> Milano, Italy and the Department of Pathology and Laboratory Medicine,<sup>†</sup> Indiana University School of Medicine, Indianapolis, Indiana

**We have investigated the proteolytic cleavage of the cellular (PrP<sup>C</sup>) and pathological (PrP<sup>Sc</sup>) isoforms of the human prion protein (PrP) in normal and prion-affected brains and in tonsils and platelets from neurologically intact individuals. The various PrP species were resolved after deglycosylation according to their electrophoretic mobility, immunoreactivity, Sarkosyl solubility, and, as a novel approach, resistance to endogenous proteases. First, our data show that PrP<sup>C</sup> proteolysis in brain originates amino-truncated peptides of 21 to 22 and 18 (C1) kd that are similar in different regions and are not modified by the PrP codon 129 genotype, a polymorphism that affects the expression of prion disorders. Second, this proteolytic cleavage of PrP<sup>C</sup> in brain is blocked by inhibitors of metalloproteases. Third, differences in PrP<sup>C</sup> proteolysis, and probably in Asn glycosylation and glycosylphosphatidylinositol anchor composition, exist between neural and non-neural tissues. Fourth, protease-resistant PrP<sup>Sc</sup> cores in sporadic Creutzfeldt-Jakob disease (CJD) and Gerstmann-Sträussler-Scheinker F198S disease brains all have an intact C1 cleavage site (Met111-His112), which precludes disruption of a domain associated with toxicity and fibrillogenesis. Fifth, the profile of endogenous proteolytic PrP<sup>Sc</sup> peptides is characteristic of each disorder studied, thus permitting the molecular classification of these prion diseases without the use of proteinase K and even a recognition of PrP<sup>Sc</sup> heterogeneity within type 2 CJD patients having different codon 129 genotype and neuropathological phenotype. This does not exclude the role of additional factors in phenotypic expression; in particular, differences in glycosylation that may be especially relevant in the new variant CJD. Proteolytic processing of PrP may play an important role in the neurotropism and phe-**

**notypic expression of prion diseases, but it does not appear to participate in disease susceptibility. (Am J Pathol 1998, 153:1561–1572)**

The prion protein (PrP) is a glycosylphosphatidylinositol (GPI)-anchored membrane protein<sup>1</sup> encoded by a gene located on chromosome 20 in humans.<sup>2</sup> PrP is expressed in many different tissues and cell types,<sup>3</sup> but the highest levels are found in neurons.<sup>4</sup> The cleavage of an amino-terminal signal peptide of 22 amino acids and 23 carboxyl-terminal residues of the polypeptide chain predicted from the cDNA sequence renders a mature product of 208 amino acids.<sup>1,5</sup> Its structure includes an amino-terminal domain with a set of octarepeats, a central hydrophobic domain, and a carboxyl-terminal region containing two Asn-linked glycosylation sites and an internal disulfide bond.<sup>4</sup> The physiological role of PrP is unknown, although it has been associated with embryonic development,<sup>6</sup> neuronal differentiation,<sup>7</sup> lymphocyte activation,<sup>8</sup> synaptic function,<sup>9</sup> circadian rhythms,<sup>10</sup> and gene transcription.<sup>11</sup>

Prion diseases are neurodegenerative disorders of humans and animals pathologically characterized by spongiosis, gliosis, neuronal loss, and variable amyloid deposition.<sup>12</sup> Human prion diseases encompass sporadic Creutzfeldt-Jakob disease (CJD); genetic forms linked to the PrP gene (*PRNP*), such as familial CJD, Gerstmann-Sträussler-Scheinker disease (GSS), and fatal familial insomnia (FFI); and infectious forms such as kuru, iatrogenic CJD, and new variant CJD.<sup>13</sup> Most of these disorders may be experimentally transmitted through exposure to pathological tissues. Extensive purification of the infectious agent of scrapie, a prototypic prion disease of sheep, led to the isolation of a major and possibly sole protein component.<sup>14</sup> Subsequent studies identified that protein as a relatively insoluble and protease-resistant abnormal PrP isoform, termed PrP<sup>Sc</sup> or PrP<sup>res</sup>.<sup>15,16</sup>

Supported by the National Institutes of Health grants AR 02594 and AG 08721 to B. Frangione, the Italian Ministry of Health, Department of Social Services and Telethon-Italy (grant E.250) to F. Tagliavini and NS29822 to B. Ghetti.

Accepted for publication July 29, 1998.

Address reprint requests to Frances Prelli, New York University Medical Center, 560 First Avenue, New York, NY 10016.

PrP<sup>Sc</sup> derives from the normal cellular form (PrP<sup>C</sup>) via a post-translational process<sup>17</sup> that is thought to lead to a conformational transition within the central hydrophobic and carboxyl-terminal regions of PrP resulting in a striking increase in  $\beta$ -sheet secondary structure.<sup>18</sup> The efficiency of this reaction may be influenced by certain amino acid substitutions in the PrP sequence, such as the codon 129 polymorphism<sup>19,20,21</sup> and the mutations linked to familial prion diseases.<sup>22</sup> The overrepresentation of PrP codon 129 homozygotes in iatrogenic and sporadic CJD as well as the restriction of new variant CJD to Met/Met subjects show that the codon 129 polymorphism affects the individual susceptibility to prion diseases.<sup>19,20,23</sup> Moreover the presence of Val or Met at codon 129 of *PRNP* in phase with the D178N mutation determines the phenotypic presentation as CJD or FFI, respectively.<sup>21</sup> Recent data suggest that distinct host molecules (factor X) also are implicated in the conversion.<sup>24</sup> The most likely candidates are PrP-binding proteins with chaperone activity,<sup>25</sup> but other alternatives cannot be excluded.

Characteristics of the proteolytic cleavage of PrP<sup>C</sup> in humans have been only partially addressed.<sup>26</sup> As particular domains appear to be relevant to the conformational change that distinguishes PrP<sup>Sc</sup> from PrP<sup>C</sup>, distinct proteolytic pathways of PrP<sup>C</sup> might yield peptides with different susceptibility to conversion.<sup>27–30</sup> Likewise, knowledge of proteolytic processing of PrP<sup>Sc</sup> isoforms is limited to the identification and characterization of fragments generated by proteinase K (PK), a nonphysiological method of cleavage. This approach has allowed a differentiation of prion disorders based on the molecular weight and degree of glycosylation of their protease-resistant PrP cores, including two types of sporadic CJD, a third type characteristic of peripherally acquired CJD, and a fourth type found only in the new variant CJD.<sup>23,31</sup> In this paper we show that the endogenous proteolytic cleavage of PrP<sup>C</sup> in normal and in Alzheimer disease (AD) control brains follows a stereotypic pattern that is similar in brain cortex and cerebellum and not modified by the codon 129 genotype. However, we found significant differences in PrP<sup>C</sup> proteolysis, and probably in glycosylation and GPI composition, between neural and non-neural (tonsils and platelets) tissues. Most remarkably, we observed characteristic proteolytic pathways in brains affected with type 1 and type 2 sporadic CJD and GSS cases carrying the F198S mutation (GSS F198S), which generated PrP<sup>Sc</sup> fragments that appear to be specific for each particular disorder.

## Materials and Methods

### Tissue Sample

Neural tissues were obtained at autopsy from 10 AD patients (AD1-10; age, 74.3  $\pm$  2.1 years; postmortem intervals of 4 to 16 hours), 9 sporadic CJD cases (CJD1-9; age, 63.5  $\pm$  6.9 years; postmortem intervals of 18 to 24 hours), 2 GSS patients carrying the F198S mutation (GSS1 and GSS2; ages 58 and 77 years; postmortem intervals of 5 and 7 hours), and 2 neurologically normal

subjects (N1 and N2; ages 74 and 78 years; postmortem intervals of 6 and 8 hours). Samples consisted of fragments of brain cortex (N1, AD1-3, AD7, AD8, CJD1-9, GSS1, and GSS2) and cerebellum (N2, AD4-6, AD9, AD10, CJD3, CDJ9, and GSS1). AD was diagnosed according to CERAD criteria.<sup>32</sup> The diagnosis of sporadic CJD and GSS was based on clinical, neuropathological, biochemical, and genetic criteria. Tonsils were collected after surgical removal from three otherwise normal children. Fresh platelets from three healthy individuals were purified by gel filtration as described.<sup>33</sup> All samples were frozen immediately after collection and stored at  $-80^{\circ}\text{C}$ .

### Molecular Genetic Analysis

DNA was extracted from brain by standard procedures and analyzed to determine the genotype at codon 129 of the PrP gene.<sup>34</sup> Polymerase chain reaction (PCR) was performed using oligonucleotide forward (5'-AAG AAG CGC CCG AAG CCT GGA GGA TGG-3') and reverse (5'-ATC CTG CAG GGG CCT GTA CAC TTG GTT-3') for 30 cycles, each consisting of a denaturation step at 94°C for 30 seconds, an annealing step at 50°C for 30 seconds, and an elongation step at 72°C for 90 seconds. PCR products of 438 bp were separated on 5% polyacrylamide gels and visualized by ethidium bromide staining. After confirming successful amplification, PCR products were digested with *Maell* (Boehringer-Mannheim, Indianapolis, IN) following the manufacturer's conditions. The resulting fragments were resolved on 5% polyacrylamide gels and visualized by ethidium bromide staining under ultraviolet light.

### Homogenization and Sarkosyl Solubility

Tissues were homogenized using a mixer pellet pestle in 6 vol of lysis buffer (10 mmol/L Tris, 150 mmol/L NaCl, 1% Nonidet P-40, 0.5% deoxycholic acid, 0.1% SDS, 5 mmol/L EDTA, pH 8) in the presence of protease inhibitors (Complete, Boehringer-Mannheim). After centrifugation at 12,000 rpm for 15 minutes, pellets were discarded and supernatants (S) were stored in aliquots at  $-80^{\circ}\text{C}$ .

To test Sarkosyl solubility tissues were homogenized in 9 vol of sucrose buffer (0.25 mmol/L sucrose, 10 mmol/L Tris, 5 mmol/L EDTA, pH 7.5). After centrifugation at 1000  $\times g$  for 10 minutes, pellets were discarded and supernatants (S1) were centrifuged again at 100,000  $\times g$  for 1 hour at 4°C. The resultant pellets (P2) were resuspended in 1 vol of TNE buffer (20 mol/L Tris, 150 mmol/L NaCl, 2 mmol/L EDTA, pH 7.5), diluted with 9 vol of the same buffer containing 2% Sarkosyl, and centrifuged at 100,000  $\times g$  for 1 hour to obtain soluble (S3) and insoluble (P3) fractions. S3 was concentrated with 4 vol of ice-cold methanol, and then both S3 precipitate and P3 were resuspended in 1 vol of TNE.

### Enzymatic Deglycosylation

Sample aliquots were mixed with 1/10 volume of denaturing buffer (20 mmol/L Tris, 150 mmol/L NaCl, 2 mmol/L

EDTA, 10%  $\beta$ -mercaptoethanol, 5% SDS, pH 7.5) and boiled for 15 minutes. After addition of Nonidet P-40 to 1%, Asn-linked oligosaccharides were cleaved by incubation with recombinant PNGase-F for 4 hours at 37°C and 12 hours at room temperature, as specified by the supplier (Biolabs, Beverly, MA).

### PK Treatment

Aliquots of S fractions were precipitated with 4 vol of ice-cold methanol. Pellets were resuspended in 1 vol of TNE and incubated with 50  $\mu$ g/ml PK (Boehringer-Mannheim) at 37°C. The reaction was stopped after 1 hour by addition of 3 mmol/L phenylmethylsulfonyl fluoride.

### Immunoblot Analysis

Sample aliquots were mixed with 1/2 volume of 3X loading buffer (240 mmol/L Tris, 6% SDS, 6%  $\beta$ -mercaptoethanol, 30% glycerol, 0.06% bromophenol blue, pH 6.8) and boiled for 5 minutes. After centrifugation at 12,000 rpm for 1 minute, samples were electrophoresed on 16.5% polyacrylamide Tris-tricine gels and electroblotted onto nitrocellulose membranes for 1 hour at 400 mA using 10 mmol/L 3-cyclohexylamino-1-propanesulfonic acid buffer, pH 11, containing 10% methanol. The membranes were blocked with 5% nonfat dried milk in TBST (10 mmol/L Tris, 150 mmol/L NaCl, 0.1% Tween 20, pH 7.5) for 2 hours at room temperature and then incubated under the same conditions with antibodies 3F4 or  $\alpha$ -SP214 diluted 1:50,000 and 1:100, respectively. 3F4 is a monoclonal antibody directed to human PrP residues 109 to 112.<sup>35</sup>  $\alpha$ -SP214 is a monoclonal antibody raised against a synthetic peptide corresponding to human PrP residues 214 to 231 that was synthesized and characterized by analytical reverse-phase high-pressure liquid chromatography, amino acid analysis, and desorption spectrometry by Chiron Corp. (Emeryville, CA). The monoclonal antibody to this peptide was custom produced by the Tissue Culture/Hybridoma Facility at State University of New York (Stony Brook, NY). The membranes were washed with TBST and then incubated for 1 hour with a horseradish-peroxidase-conjugated rabbit anti-mouse antibody (Amersham, Arlington Heights, IL) at a dilution of 1:5000. The membranes were washed again, developed using an enhanced chemiluminescent substrate (SuperSignal, Pierce, Rockford, IL), and detected with autoradiography film (Reflection, Dupont NEN, Boston, MA). For quantitative analyses, blots were scanned using the UMAX 2.4.1 Magic Scan, and the density of the bands was measured using NIH Image software.

### Protease Inhibition

Aliquots of normal brain cortex (N1) sucrose homogenate were diluted with 5 vol of phosphate-buffered saline, pH 7.2, incubated at 37°C for 24 hours with protease inhibitors (Table 1), metal ions ( $\text{Ca}^{2+}$ ,  $\text{Cu}^{2+}$ ,  $\text{Fe}^{2+}$ ,  $\text{Mg}^{2+}$ , or  $\text{Zn}^{2+}$ ), or both at a 20:1/inhibitor:metal ion molar ratio and then deglycosylated and analyzed by immunoblot with

Table 1. Protease Inhibitors and Concentrations Applied

I. Metalloproteinases	
EDTA	5 mmol/L
EGTA	10 mmol/L
1,10-o-phenanthroline	5 mmol/L
Phosphoramidon	1 mmol/L
II. Aspartylproteinase	
Pepstatin A	2.5 mg/ml
III. Thiolproteinases	
PCMBs	50 mmol/L
E-64	1 mmol/L
Cystatin A	0.1 mg/ml
$\alpha_2$ -Macroglobulin	1 mg/ml
IV. Amino/carboxyproteinases	
Bestatin	1 mmol/L
Captopril	1 mmol/L
V. Serine proteinases	
Benzamidine	2.5 mmol/L
PMSF	2 mmol/L
Aprotinin	1 mg/ml
TLCK	1 mmol/L
Leupeptin	0.2 mmol/L
Soybean Trypsin Inhibitor	0.5 mg/ml
DFP <sup>4</sup>	100 $\mu$ -mol/L

PCMBs, *p*-chloromercuricbenzenesulfonic acid; PMSF, phenylmethanesulfonyl fluoride; TLCK, N<sup>α</sup>-tosyl-lys-chloromethyl ketone hydrochloride; DFP<sup>4</sup>, diisopropylfluorophosphate.

antibody  $\alpha$ -SP214. The bands corresponding to full-length PrP were quantified by densitometry, and the results were expressed as a percentage related to the control, a nonincubated aliquot.

## Results

### Amino-Truncated Fragments of 21 to 22 and 18 kd Are the Major Proteolytic Products of the PrP<sup>C</sup> Isoform in Normal and AD Brains

To study the proteolytic processing of PrP<sup>C</sup> in brain we analyzed 10 AD and 2 normal autopsy brains. The basis for the selection of AD brains was, namely, 1) the absence of detectable levels of PrP<sup>Sc</sup> in AD brains<sup>36</sup> and 2) the existence of specific and widely accepted diagnostic criteria for AD.<sup>32</sup> As the polymorphism at codon 129 of the PrP gene affects the phenotypic expression of prion disorders and the susceptibility to particular strains,<sup>19,20,21,23,31</sup> we compared the different genotypes: 1) N2 and AD cases 4, 5, 7, and 10 were heterozygous Met/Val; 2) N1 and AD cases 2, 3, 8, and 9 were homozygous for Met; and 3) AD cases 1 and 6 were homozygous for Val.

The AD and normal brains were tested by immunoblot analysis with 3F4 and  $\alpha$ -SP214, two monoclonal antibodies directed to the central (residues 109 to 112) and carboxyl-terminal (residues 214 to 231) regions of human PrP, respectively. In contrast to these domains, the amino-terminal region of PrP is labile and not needed for infectivity.<sup>37</sup> Sample aliquots were standardized to yield signals of approximately equal intensity in immunoblots probed with 3F4; these quantities were employed in all assays.

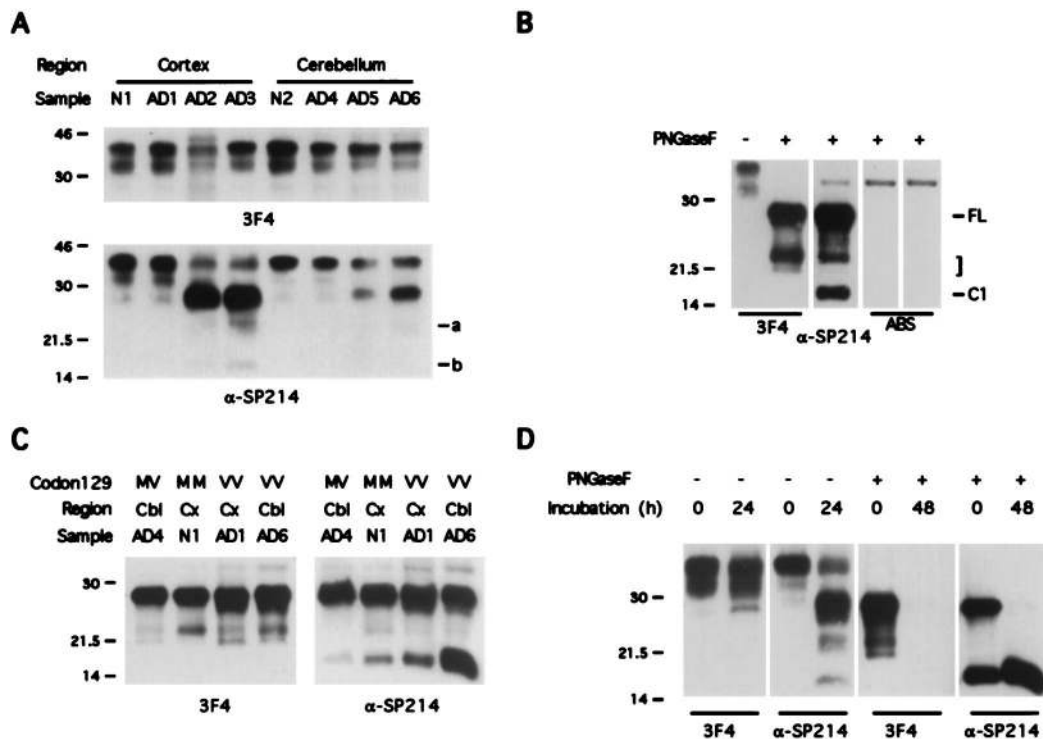


**Figure 1.** Characteristics of the PrP<sup>C</sup> isoform in normal and AD brains. **A:** Immunoblot analysis of brain cortex and cerebellum from two neurologically normal individuals (N1 and N2) and six AD patients (AD1–6), using anti-PrP monoclonal antibodies 3F4 and  $\alpha$ -SP214. The signal above the 37-kd band in 3F4 blots is nonspecific. **a** and **b** indicate two bands of 22 and 18 kd, respectively, detected only with  $\alpha$ -SP214. **B:** Immunoblot analysis of normal brain (N1) with 3F4,  $\alpha$ -SP214, and the same antibodies after preabsorption (ABS). Samples were treated (+) or untreated (–) with PNGase-F. The labels show the position of full-length PrP (FL) and amino-truncated fragments of 21 to 22 and 18 (C1) kd. **C:** Immunoblot analysis of four representative deglycosylated normal (N1) and AD (AD cases 1, 4, and 6) brain homogenates probed with 3F4 and  $\alpha$ -SP214. Samples include neocortical (Cx) and cerebellar (Cbl) tissues from subjects with Met/Val (MV), Met/Met (MM), and Val/Val (VV) PrP codon 129 genotypes. **D:** Effects of endogenous proteases on the PrP<sup>C</sup> isoform in brain. Normal brain cortex (N1) was incubated for 24 to 48 hours at room temperature, homogenized, treated (+) or untreated (–) with PNGase-F, and analyzed by immunoblot with antibodies 3F4 and  $\alpha$ -P214. Numbers on the left correspond to the molecular weight markers in kilodaltons.

Untreated AD and normal brain homogenates tested with 3F4 contained two broad immunoreactive bands of 35 and 33 kd and a faint band of 27 kd (Figure 1A). All samples exhibited a similar 3F4 pattern characterized by a decreasing intensity from high to lower molecular weight bands. However, the immunoblots developed with  $\alpha$ -SP214 showed a marked heterogeneity (Figure 1A). Eight samples (N1, N2, and AD cases 1, 4, and 7 to 10) had a pattern comparable to that with 3F4 (pattern 1). The remaining cases (AD cases 2, 3, 5 and 6) contained major bands of 35 and 27 kd (pattern 2) and two fainter signals at 22 and 18 kd (Figure 1A). The postmortem intervals of all pattern 2 samples were longer than 8 hours (range, 8 to 16 hours), whereas pattern 1 cases had intervals of 4 to 10 hours.

After deglycosylation, immunoblot analysis of the 10 AD and 2 normal brains showed a major broad band of 27 kd and various species of 21 to 22 kd when probed with 3F4 and an additional carboxyl-terminal fragment of 18 kd when probed with  $\alpha$ -SP214 (Figure 1B). The 27-kd band is consistent with the molecular weight of deglycosylated full-length PrP,<sup>38</sup> whereas the remaining signals correspond to amino-truncated fragments.<sup>26</sup> The 35- and 33-kd bands were not detected after PNGase-F treatment, which indicates that they are glycosylated species. There were no significant molecular weight differences between the deglycosylated PrP<sup>C</sup> fragments of normal

and AD brains or of different PrP codon 129 genotypes or of neocortical and cerebellar tissues (Figure 1C). However, there was an obvious heterogeneity in the intensity of the 18-kd band, with pattern 2 samples presenting a higher signal than pattern 1 cases (Figure 1C, AD6). The intensity of the 21 to 22-kd bands appeared to vary randomly with the immunoblot profile of untreated homogenates.

As pattern 2 samples had longer postmortem intervals and a proportionally higher content of 18-kd fragment than pattern 1 cases, we suspected that the observed differences were related to postmortem lysis. To address the endogenous proteolysis of the PrP<sup>C</sup> isoform, intact normal and AD brain tissues were incubated for 24 to 48 hours at room temperature before homogenization. Brain samples thus treated showed a progressive increase in the deglycosylated 18-kd fragment and a concomitant decrease in the 27- and 21- to 22-kd species (see the example of N1, a pattern 1 case, in Figure 1D). These quantitative changes reflected a conversion of pattern 1 to pattern 2 (Figure 1D).

#### *Metalloproteases Are Involved in the Proteolytic Processing of PrP<sup>C</sup> in Brain*

Taking advantage of the effects of postmortem lysis, we then tried to identify the enzymatic activities involved in



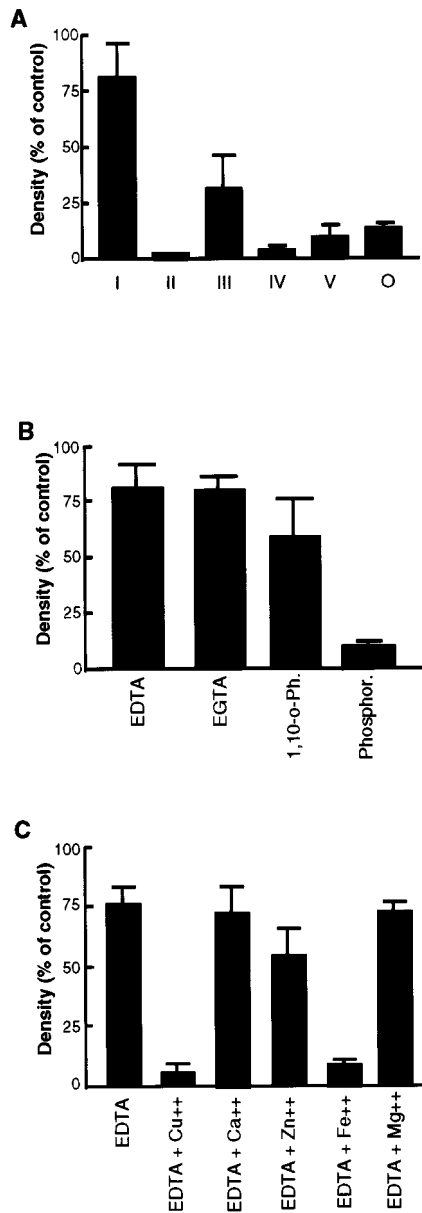


**Figure 2.** Enzymatic activities involved in PrP<sup>C</sup> proteolysis in brain homogenates. Aliquots of normal brain cortex (N1) sucrose homogenate were incubated at 37°C for 24 hours with protease inhibitors (Table 1), metal ions, or both, deglycosylated, analyzed by immunoblot with antibody  $\alpha$ -SP214, and quantified by densitometry. Herein we show the mean and standard deviation of three independent experiments. **A:** Effect of different combinations of protease inhibitors. Roman numbers refer to the groups of protease inhibitors listed in Table 1. O, sample incubated in the absence of inhibitors. **B:** Effect of different inhibitors of metalloproteases. 1-10-o-Ph, 1,10-o-phenanthroline; Phosphor., phosphoramidon. **C:** Effect of metal ions. Divalent metal ions (Ca<sup>2+</sup>, Mg<sup>2+</sup>, Fe<sup>2+</sup>, Cu<sup>2+</sup>, and Zn<sup>2+</sup>) were added to EDTA-containing aliquots at a 20:1 EDTA:metal ion molar ratio.

PrP<sup>C</sup> degradation. Aliquots of normal brain (N1) homogenate were incubated for 24 hours at 37°C in the presence of different protease inhibitors (Table 1), deglycosylated, and analyzed by immunoblot with  $\alpha$ -SP214. The 27-kd bands corresponding to full-length PrP were quantified by densitometry, and results were expressed as percentage of intensity related to control, not incubated samples. As shown in Figure 2, A and B, the metal-

chelating agents EDTA and EGTA were the most effective in blocking PrP<sup>C</sup> degradation. The effect of EDTA was reversed by adding divalent metal ions (Ca<sup>2+</sup>, Mg<sup>2+</sup>, Fe<sup>2+</sup>, Cu<sup>2+</sup>, and Zn<sup>2+</sup>) in molar excess (not shown), but only Fe<sup>2+</sup>, Cu<sup>2+</sup>, and to a far lesser degree Zn<sup>2+</sup> were active when added at a 20:1/EDTA:metal ion molar ratio (Figure 2C).

### *Sporadic CJD and GSS F198S Brains Exhibit Characteristic PrP Proteolytic Pathways*

Prion disease brains contain both PrP<sup>C</sup> and PrP<sup>Sc</sup> isoforms, which can be differentiated by the relative PK resistance and insolubility in nondenaturing detergents of the latter.<sup>14,16</sup> Our sporadic CJD cases could be divided into two groups by the size of their PK-resistant cores.<sup>23,31</sup> Four cases (CJD1 to -3 and CJD7), all of them homozygous for Met at codon 129, contained three bands of 31, 28, and 22.5 kd in blots probed with 3F4 and  $\alpha$ -SP214, corresponding to di-, mono-, and unglycosylated species, respectively (type 1 sporadic CJD; Figure 3, A and B). A second group included cases with Met/Val (CJD4 and CJD9), Met/Met (CJD6), and Val/Val (CJD5 and CJD8) genotypes, and in each case the PK-treated samples had similar bands of 30, 26, and 21 kd (type 2 sporadic CJD; Figure 3, A and B). The patterns of our type 1 and type 2 sporadic CJD groups were in agreement with type 1 and type 2 PrP<sup>res</sup><sup>31</sup> although with minor differences in electrophoretic mobility, probably due to experimental variability. PK-treated GSS F198S brain tissue (GSS1 and GSS2, both with Met/Val codon 129 genotype) contained bands of 27 to 29, 18 to 20, and 8 kd detectable only by 3F4 and a faint 33-kd signal revealed by both antibodies (Figure 3A).<sup>39</sup> As expected, protease-resistant species in CJD and GSS brains were similar in cortical and cerebellar tissues and insoluble in 2% Sarkosyl (not shown), whereas PK treatment of normal and AD brains led to a lack of immunoreactive bands in blots probed with both 3F4 and  $\alpha$ -SP214 (Figure 3A).

Two important limitations of PK treatment of PrP are the nonphysiological cleavage, which precludes the identification of naturally occurring species, and the observed variable PK resistance of PrP<sup>Sc</sup> isoforms in different prion disorders, which may be minimal in some cases.<sup>40</sup> To investigate the spectrum of PrP species in prion disease brains, we used an alternative approach based on deglycosylation, resistance to endogenous proteases and Sarkosyl solubility. Deglycosylation alone allows identification of the full range of proteolytic fragments, whereas insolubility in nondenaturing detergents and resistance to endogenous proteases may differentiate PrP<sup>Sc</sup> from PrP<sup>C</sup> isoforms without PK digestion.

After deglycosylation, type 1 sporadic CJD brain cortex and cerebellum had species of 27 and 22.5 kd detectable by 3F4 and  $\alpha$ -SP214 and an 18-kd fragment detected only with  $\alpha$ -SP214 (Figure 4, A and B).<sup>26</sup> The pattern of deglycosylated type 2 CJD samples was indistinguishable from that of normal and AD brains (Figure 4, A and B), except for the presence of PrP aggregates in tissues with high amyloid content (Figure 5B). GSS F198S

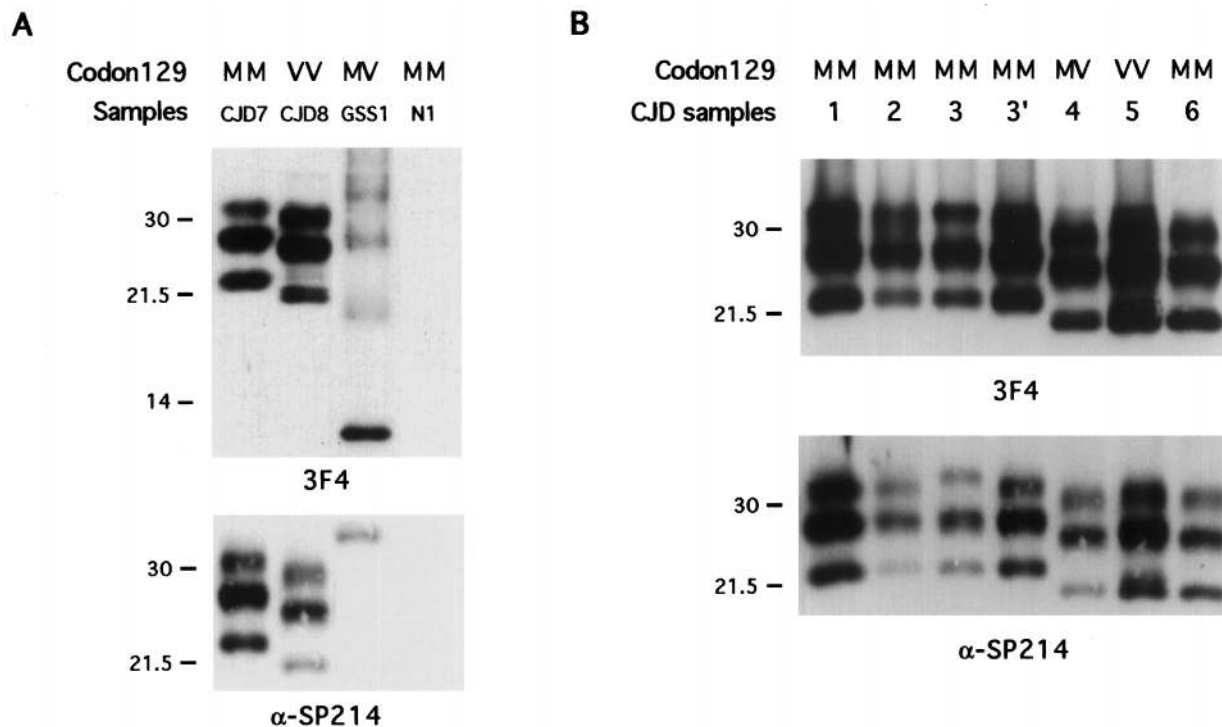


**Figure 3.** PK-resistant PrP<sup>Sc</sup> cores in sporadic CJD and GSS F198S brains. PK-treated homogenates were tested by immunoblot using antibodies 3F4 and  $\alpha$ -SP214. **A:** Comparative analysis of brain cortex samples from type 1 (CJD7) and type 2 (CJD8) sporadic CJD cases and one GSS F198 patient (GSS1). Note the lack of PK-resistant PrP in a normal control brain (N1). **B:** Analysis of a series of type 1 (CJD1–3') and type 2 (CJD4–6) sporadic CJD cases. All samples are from brain cortex except 3', which corresponds to cerebellum from case CJD3. MV, VV, and MM, Met/Val, Val/Val, and Met/Met codon 129 genotypes, respectively. Numbers on the left correspond to the molecular weight markers in kilodaltons.

brains had a distinctive 3F4 profile, composed of peptides measuring 27 to 30, 21 to 22, 19 to 20, and 9 kd, and a diffuse high molecular weight signal (Figure 4A).<sup>39</sup> GSS samples tested with  $\alpha$ -SP214 contained species of 27 to 30, 21 to 22, and 18 kd.

To analyze the effects of endogenous proteases on the PrP<sup>Sc</sup> isoforms of CJD and GSS F198S brains, intact tissue samples were incubated at room temperature for 24 hours before homogenization and deglycosylation. Type 1 sporadic CJD cases showed a decrease in full-length PrP with a concomitant increase in the 22.5- and 18-kd fragments (Figure 4C). The results of type 2 CJD brains were more heterogeneous. Cerebral cortex from Val/Val patients mirrored the profile of normal brain, with a decrease in full-length PrP and 21- to 22-kd species and an increase in the 18-kd peptide (Figure 4C). In contrast, tissues from a Met/Val case with high amyloid burden presented higher amounts of the 21- to 22-kd fragments (Figure 4D). GSS F198S samples had a decrease in full-length PrP and 21- to 22-kd species and an increase in the 20- and 9-kd peptides; in addition, a carboxyl-terminal fragment of 10 kd was detected (Figure 4C).

To further discriminate between PrP<sup>C</sup> and PrP<sup>Sc</sup> in CJD and GSS brains, tissues were homogenized in 2% Sarkosyl, centrifuged to obtain soluble and insoluble fractions, and deglycosylated. The soluble fractions of type 1 sporadic CJD brains contained a small quantity of full-length PrP and all of the detectable 18-kd fragment. The insoluble fractions, enriched in PrP<sup>Sc</sup>, included the majority of full-length PrP and the 22.5-kd fragment (Figure

5A). The soluble fractions of type 2 CJD brains contained intact PrP and fragments of 21 to 22 and 18 kd, whereas the insoluble fractions included PrP aggregates, full-length PrP, and 21- to 22-kd products (Figure 5, A and B). Of note, the relative amounts of PrP in each fraction were again more heterogeneous in type 2 than in type 1 CJD. Type 2 CJD samples with high amyloid content, such as cerebellum from Met/Val heterozygotes, had the greatest quantities of insoluble PrP (Figure 5B), whereas brain cortex from Val/Val patients contained minimal amounts of insoluble PrP, mainly in the form of full-length species (Figure 5a, CJD8). These results correlate with those of PrP degradation by endogenous proteases and may be explained by the reported variation of PrP<sup>res</sup> content in type 2 CJD tissues.<sup>31</sup> Comparable assays using GSS F198S brains showed the presence of full-length PrP and the 21- to 22- and 18-kd fragments in the supernatants; the pellets contained the bulk of the immunoreactive material, composed of PrP aggregates, full-length PrP, and truncated products of 19 to 20 and 9 kd (Figure 5A).

#### *Tissue-Specific Properties of the PrP<sup>C</sup> Isoform in Non-Neural Tissues*

The mechanisms controlling the neurotropism of prions are still unclear. As prion replication requires a PrP<sup>C</sup>-PrP<sup>Sc</sup> interaction that is affected by homology,<sup>41</sup> tissue-specific attributes of PrP<sup>C</sup> may modulate, and eventually preclude, the pathological conversion. Lymphoid tissue

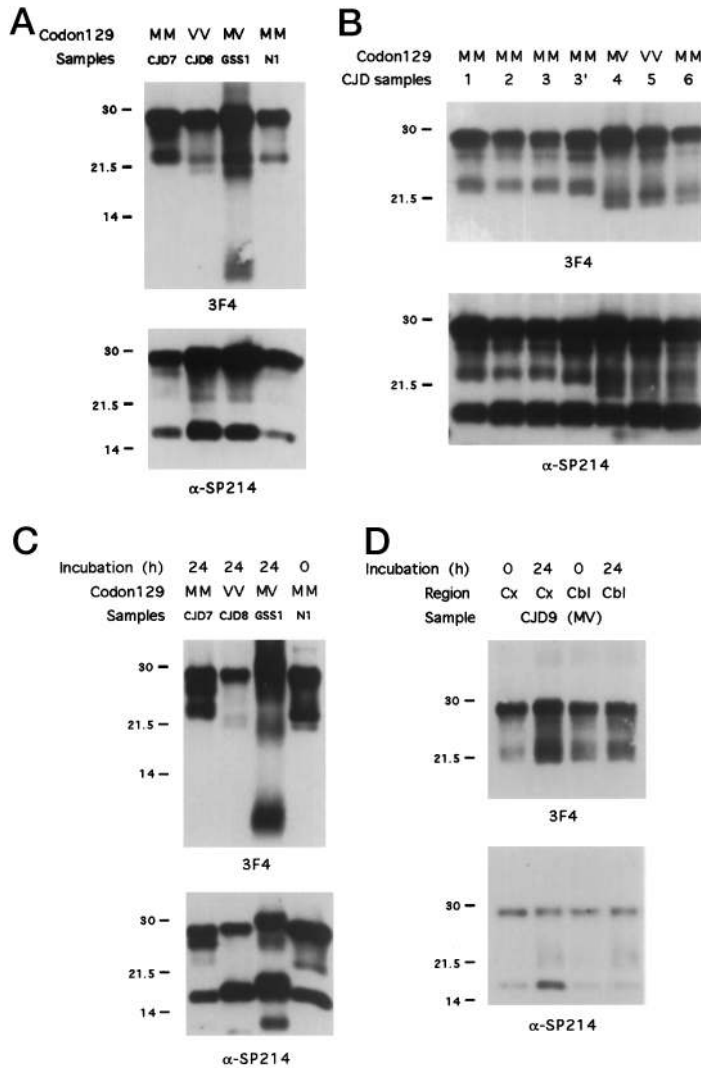


**Figure 4.** PrP proteolytic fragments in sporadic CJD and GSS F198S brains. **A:** Comparative analysis of deglycosylated brain cortex homogenates from type 1 (CJD7) and type 2 (CJD8) sporadic CJD cases and a GSS F198S patient (GSS1). Samples were analyzed by immunoblot using monoclonal antibodies 3F4 and  $\alpha$ -SP214. A normal brain (N1) is included for comparison. **B:** Analysis of a series of type 1 (CJD1–3') and type 2 (CJD4–6) sporadic CJD cases. All samples are from brain cortex except 3', which corresponds to cerebellum from case CJD3. Tissues were analyzed as described in **A**. **C:** Effects of endogenous proteases in the PrP species of sporadic CJD and GSS F198S brains. Brain cortex samples from type 1 (CJD7) and type 2 (CJD8) sporadic CJD cases and a GSS F198S patient (GSS1) were incubated at room temperature for 24 hours, homogenized, deglycosylated, and analyzed by immunoblot with monoclonal antibodies 3F4 and  $\alpha$ -SP214. These data should be compared with those in **A**, which present the profile of the same cases before incubation. A normal brain not incubated (N1) is included as control. **D:** Effects of endogenous proteases on the PrP species of cortical (Cx) and cerebellar (Cbl) samples from a type 2 sporadic CJD Met/Val case (CJD9) with extensive PrP amyloid deposition. The analysis was performed as described in **C**. MV, VV, and MM, Met/Val, Val/Val, and Met/Met codon 129 genotypes, respectively. Numbers on the left correspond to the molecular weight markers in kilodaltons.

(tonsils) and platelets have significant amounts of PrP.<sup>8,42</sup> Immunoblot analysis of untreated homogenates of platelets and tonsils from neurologically normal subjects revealed three 3F4 and  $\alpha$ -SP214 immunoreactive bands of 38, 33, and 26 kd (Figure 6A). Fully glycosylated platelet and tonsil PrP<sup>C</sup> had a higher molecular weight than the brain homologue. Conversely, deglycosylated, full-length PrP<sup>C</sup> in non-neural tissues had a lower molecular weight (approximately 26 kd) than in brain (27 kd; Figure 6B). Tonsil samples contained additional deglycosylated fragments of 20 to 21 kd detected with 3F4 and minimally with  $\alpha$ -SP214 and an 18-kd fragment detectable only by  $\alpha$ -SP214 (Figure 6B). Deglycosylated platelet PrP<sup>C</sup> fragments were identified at 16 kd with  $\alpha$ -SP214 and at 19 kd with both 3F4 and  $\alpha$ -SP214 (Figure 6B).

### Discussion

A central pathogenic event in prion disorders is a conformational transition of PrP from a normal cellular isoform (PrP<sup>C</sup>) to a pathological species (PrP<sup>Sc</sup>) enriched in  $\beta$ -sheet structure.<sup>18</sup> Recent data show that this conver-

sion may be modulated by a host of factors. First, amino acids in the PrP sequence, such as the polymorphic residue 129 in humans, influence the phenotypic expression of prion diseases and the susceptibility to particular strains through a yet unknown mechanism.<sup>19,20,21,23,31,43</sup> The most striking indication of the role of this factor is the observed restriction of new variant CJD to individuals homozygous for Met at codon 129 of the PrP gene. Second, PrP mutations have been linked to familial prion disorders, which suggests that they directly lead to pathogenic conformational changes.<sup>22</sup> Third, species-specific PrP-binding macromolecules, provisionally termed protein X, may modulate the PrP<sup>C</sup>-PrP<sup>Sc</sup> interaction.<sup>24</sup> It has been postulated that amyloid-associated proteins may be acting as pathological molecular chaperones that induce  $\beta$ -pleated sheet conformation in amyloidogenic peptides.<sup>44</sup> Fourth, protein Y, an unknown product encoded by a gene other than *PRNP*, appears to be involved in the distribution of lesions in scrapie-infected mice.<sup>45</sup> Fifth, changes in environmental conditions such as pH may induce major modifications in the secondary structure of PrP.<sup>46</sup> Despite these data, the exact

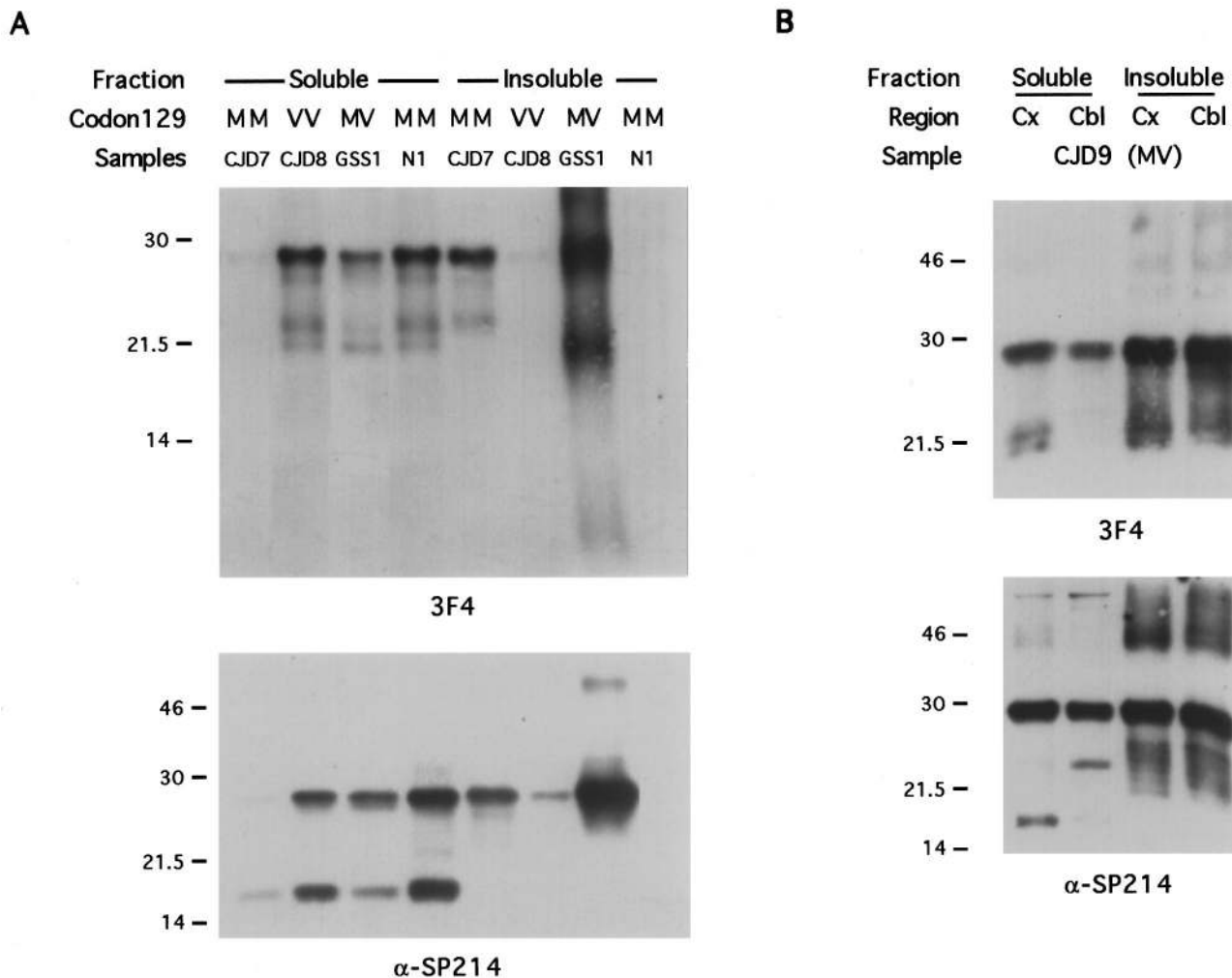


**Figure 5.** Solubility of the PrP species of sporadic CJD and GSS F198S brains. Tissues were homogenized in 2% Sarkosyl and ultracentrifuged to obtain soluble and insoluble fractions, which then were deglycosylated and analyzed by immunoblot using antibodies 3F4 and  $\alpha$ -SP214. **A:** Comparative analysis of brain cortex samples from type 1 (CJD7) and type 2 (CJD8) sporadic CJD cases and a GSS F198 patient (GSS1). A normal brain (N1) is included as control. **B:** Analysis of brain cortex (Cx) and cerebellum (Cbl) from a type 2 sporadic CJD Met/Val case (CJD9) pathologically characterized by extensive PrP amyloid deposition. MV, VV, and MM, Met/Val, Val/Val, and Met/Met codon 129 genotypes, respectively. Numbers of the left correspond to the molecular weight markers in kilodaltons.

mechanism of this process is still enigmatic, and most likely other contributory factors will be identified. Specifically, we studied the proteolytic cleavage of PrP isoforms in normal, AD, sporadic CJD, and GSS F198S brains as well as in lymphoid tissue (tonsils) and platelets from neurologically normal individuals.

Different PrP<sup>C</sup> proteolytic pathways may originate fragments with distinct susceptibility to conversion, as prediction models,<sup>28</sup> comparative structural and immunological studies of PrP<sup>C</sup> and PrP<sup>Sc</sup>,<sup>18,29</sup> and nuclear magnetic resonance experiments with recombinant PrP<sup>30,47,48</sup> suggest that only certain PrP domains, especially residues 90 to 125, are essential for the conformational changes that differentiate PrP<sup>Sc</sup> from PrP<sup>C</sup>. Cleavages within these critical regions could preclude the conversion of PrP<sup>C</sup> into PrP<sup>Sc</sup>. Therefore, studies of PrP<sup>C</sup> proteolytic processing may help elucidate the phenomena of disease susceptibility and tissue specificity.

The present study shows the existence of two major PrP<sup>C</sup> proteolytic cleavages in normal and AD brain cortex

and cerebellum (Figure 7). The cleavage sites were identified by immunoblot analysis of deglycosylated samples using monoclonal antibodies 3F4 and  $\alpha$ -SP214, which revealed a spectrum of PrP fragments besides the full-length GPI-containing species of 27 kd.<sup>38</sup> We inferred that these assays reflect proteolysis because the entire open reading frame of the human PrP gene is contained within a single exon, which excludes mRNA splicing.<sup>49</sup> The dominant cleavage yields a carboxyl-terminal fragment of 18 kd that does not include the 3F4 epitope; thus, it is amino truncated and starts after Met109. This fragment has been previously denominated C1 and its amino terminus identified as His111-Met112 in neuroblastoma cell lines.<sup>26</sup> The second pathway yields heterogeneous peptides of 21 to 22 kd that contain both 3F4 and  $\alpha$ -SP214 epitopes and therefore are also amino truncated but start before or at Met109. Molecular weight estimates by immunoblot analysis suggest that the amino termini of these fragments are within residues 80 to 100. It remains to be established whether both pathways are indepen-



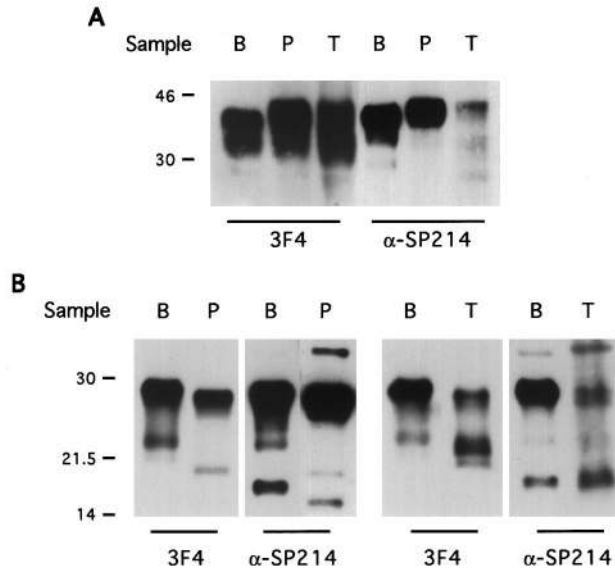


**Figure 6.** Characteristics of the PrP<sup>C</sup> isoform of platelets and tonsils from neurologically normal individuals. **A:** Immunoblot analysis of untreated platelet (P) and tonsil (T) homogenates using antibodies 3F4 and α-SP214. A normal brain cortex (B, case N1) is included as control. **B:** Immunoblot analysis of deglycosylated brain (B), platelet (P), and tonsil (T) homogenates using antibodies 3F4 and α-SP214. Numbers on the left correspond to the molecular weight markers in kilodaltons.

dent or whether the 21- to 22-kd species are obligatory intermediaries for the generation of C1 (Figure 7). In addition to the major internal cleavages, the bands adjacent to full-length PrP<sup>C</sup> in blots probed with 3F4 and α-SP214 indicate the existence of products with limited amino- and carboxyl-terminal truncation.

The presence of AD pathology apparently does not modify the cerebral proteolysis of PrP<sup>C</sup>, as we obtained equivalent immunoblot profiles of normal and sporadic AD brains. Within the limits of resolution of our assays, the results were also qualitatively similar in all of the AD and normal brains irrespective of their PrP codon 129 genotypes as well as in samples of brain cortex and cerebellum. Although we found marked differences in the relative amounts of C1 fragment, the progressive increase in C1

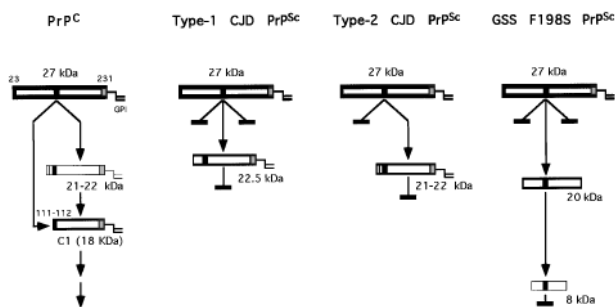


**Figure 7.** Proposed major PrP proteolytic cleavages in normal, type 1, and type 2 sporadic CJD and GSS F198S brains. Polypeptide chains of full-length PrP and several proteolytic fragments identified in normal and prion-affected brains are schematically represented (molecular weights correspond to the deglycosylated species). Data are based on the current study and previous reports.<sup>26,39</sup> Black and gray boxes mark the epitopes of monoclonal antibodies 3F4 (residues 109 to 112) and α-SP214 (within residues 214 to 231), respectively. (Arrows indicate active cleavages, while solid bars represent inactive, blocked cleavages.)

content in samples incubated without protease inhibitors shows that they were related to endogenous proteolysis. The increase in C1 concomitant with the decrease in full-length PrP and the 20- to 21-kd fragments also indicates a remarkable resistance to degradation of the carboxyl-terminal region of PrP<sup>C</sup>. Despite the changes induced by postmortem lysis, the identification of comparable fragments in brain biopsy tissue and in neuroblastoma cells<sup>26,50,51</sup> supports the existence *in vivo* of the various cleavages. As there are no major differences in the profile of PrP<sup>C</sup> fragments between brain cortex and cerebellum, or between different individuals, physiological disparities in the proteolytic processing of PrP<sup>C</sup> in brain appear neither to play a significant role in disease susceptibility nor to be involved in the particular distribution of lesions in the distinct prion disorders.

As a first attempt to characterize the enzymatic activities involved in the proteolysis of PrP<sup>C</sup> in brain, we asked which protease inhibitors are most effective in blocking PrP<sup>C</sup> degradation. The metal-chelating agents EDTA and EGTA showed the highest activity against PrP<sup>C</sup> protease(s), followed by the inhibitors of thiol proteases. The addition of Fe<sup>2+</sup> or Cu<sup>2+</sup> at a 20:1/EDTA:metal ion molar ratio reversed the effect of EDTA, indicating the selectivity of the inhibition. Although our results were reproducible, they should be interpreted cautiously because we used whole-brain homogenates, which contain a multiplicity of enzymes not necessarily relevant under physiological conditions. However, the presence of metal-binding properties of PrP, an intriguing and recurrent observation in the literature, may influence PrP conformation.<sup>52</sup> Our data also suggest a role for metal ions in the proteolytic processing of PrP. The high ferritin accumulation in microglial cells surrounding PrP amyloid plaques<sup>53</sup> could reflect among other functions the overregulation of metalloproteases involved in amyloid formation or degradation.

In contrast to the stereotypic characteristics of PrP<sup>C</sup> in normal and AD brains, we found that the PrP<sup>Sc</sup> isoforms in different prion disorders are heterogeneous. Initially, as previously reported,<sup>23,31</sup> we observed that the different molecular weights of the PK-resistant PrP<sup>Sc</sup> cores (PRP27–30) in sporadic CJD brains correlated with their codon 129 genotypes. A group of CJD cases, homozygous for Met at codon 129, had three PK-resistant bands of 31, 28, and 22.5 kd, corresponding to di-, mono-, and unglycosylated PrP species, respectively. A second group of CJD samples, composed of Met/Val, Met/Met, and Val/Val codon 129 genotypes, contained proteins of 30, 26, and 21 kd. Thus, our first and second groups correspond to the type 1 and type 2 PrP<sup>res</sup>, respectively, described by Parchi et al in sporadic CJD.<sup>31</sup> Of note, the deglycosylated 21-kd fragment described above in normal and AD brains has the same mobility and immunoreactivity as the unglycosylated PK-resistant core of type 2 CJD brain tissue; therefore, it is a physiological PrP27-30-like species. GSS F198S brains, characterized by PrP amyloid deposition associated with neurofibrillary tangles, had four PK-resistant bands of 33, 27 to 29, 18 to 20, and 8 kd.<sup>39</sup>

However, a significant limitation of PK digestion is that it is an unphysiological hydrolytic process that yields enzymatic end-products and no elucidative intermediary species. Thus, it cannot be used to characterize naturally occurring PrP species, nor does it allow study of effects of disease on PrP<sup>C</sup>. To investigate the full spectrum of PrP isoforms in prion-affected brains we used an alternative approach based on deglycosylation, degradation by endogenous proteases, and Sarkosyl solubility. Deglycosylation alone allows the identification of the multiplicity of PrP peptides present in tissues, and PrP<sup>Sc</sup> isoforms can be further distinguished by their relative protease resistance and insolubility in nondenaturing detergents.<sup>15,16</sup>

According to our data, type 1 sporadic CJD PrP<sup>Sc</sup> species are in the form of full-length PrP and a prominent amino-truncated fragment of 22.5 kd (molecular weights refer to deglycosylated species) (Figure 7). This 22.5-kd product has the same mobility and immunoreactivity as the C2 fragment identified by Chen et al in sporadic CJD brains<sup>26</sup> and represents a natural proteolytic product that coincides with the protease-resistant core obtained after PK digestion. In contrast, we describe for the first time type 2 sporadic CJD PrP<sup>Sc</sup> in the form of full-length PrP and variable amounts of amino-terminal-truncated fragments of 21 to 22 kd and PrP aggregates (Figure 7). These 21- to 22-kd products cannot be distinguished by size from homologue species of normal and AD brains, which suggests that PrP<sup>Sc</sup> proteolytic pathways in type 2 CJD are similar, if not identical, to those of PrP<sup>C</sup> in normal brain. However, whereas normal PrP<sup>C</sup> is readily cleaved further at the amino-terminus to yield the C1 fragment, PrP<sup>Sc</sup> isoform in type 2 CJD is not degraded as efficiently and eventually may accumulate as a 21-kd protease-resistant core. Interestingly, type 2 CJD cases with Met/Val codon 129 genotype and marked amyloid deposition contained higher amounts of PrP aggregates and 21- to 22-kd peptides than Val/Val cases with no or minimal amyloid accumulation. These data show that the exact profile of PrP<sup>Sc</sup> peptides in prion-affected tissues, including the relative amounts of the different species and not merely the characteristics of the protease-resistant cores, correlates with the neuropathological phenotype.

The most distinctive profile was found in GSS F198S brain tissue, which included PrP<sup>Sc</sup> aggregates, full-length PrP<sup>Sc</sup>, and amino- and carboxyl-terminal truncated fragments of 19 to 20 and 9 kd (Figure 7). Although the 22.5-kd fragment in type 1 CJD and the 19- to 20- and 9-kd products in GSS F198S brains were not found in significant amounts in normal tissue, that does not necessarily imply that they proceed from novel pathogenic cleavages. They may represent normally transient proteolytic intermediaries that are stabilized under pathological conditions. In addition to PrP<sup>Sc</sup>, prion-affected brains also had variable quantities of PrP<sup>C</sup> species, which were identified by their solubility in Sarkosyl and a normal proteolytic pattern characterized by an increase in C1 after incubation without protease inhibitors.

Taken together, our data demonstrate that the PrP<sup>Sc</sup> isoforms of different prion disorders have both common and distinct properties. First, the protease-resistant cores in sporadic CJD and GSS F198S brains were all detect-

able by 3F4, indicative of the intactness of the C1 cleavage site (His111-Met112). This holds even for the smallest amino- and carboxyl-truncated fragments of 7 and 11 kd present in GSS F198S amyloid.<sup>54,55</sup> Therefore, a pivotal difference between PrP<sup>C</sup> and PrP<sup>Sc</sup> isoforms appears to be the increased resistance to cleavage of the C1 site of PrP<sup>Sc</sup> species. The preservation of the C1 site, presumably reflective of the pathological conformation of the abnormal proteins, precludes the disruption of a conserved hydrophobic region (residues 106 to 126) involved in toxicity and fibrillogenesis<sup>56,57</sup> and may lead to reduced clearance and subsequent accumulation of deleterious PrP species. This hypothesis is supported by recent structural data that indicate that the 90 to 112 PrP<sup>C</sup> region has no defined structure<sup>30</sup> and thus may be a critical domain for the conformational change that differentiates PrP<sup>Sc</sup> from PrP<sup>C</sup>.

In contrast to this common feature of the PrP<sup>Sc</sup> isoforms, we observed characteristic proteolytic cleavages that originated fragments specific for each disorder. The possible implications of this finding are exemplified by studies of Alzheimer amyloid  $\beta$  peptide (A $\beta$ ). Amyloid A $\beta$  deposits are composed of a spectrum of peptides with heterogeneous amino and carboxy termini, derived by proteolysis from a larger precursor. Current evidence indicates that A $\beta$  variants exhibit a partially different distribution in tissues.<sup>58</sup> Previous studies of prion diseases have shown that there are differences in the molecular weight and degree of glycosylation of the PK-resistant PrP<sup>Sc</sup> cores in the distinct clinicopathological syndromes. Herein we show that there are fragments comparable to those identified after PK digestion also in intact tissues, in agreement with the results of Piccardo et al<sup>39</sup> for GSS F198S and of Chen et al<sup>26</sup> for type-1 CJD. These data indicate that the different PrP<sup>Sc</sup> isoforms, when exposed to the endogenous proteases, display patterns of cleavage that are characteristic of each disorder and therefore are associated with distinct sets of fragments. By analogy with the A $\beta$  variants, the different PrP<sup>Sc</sup> fragments may exhibit particular biological and physicochemical properties. As a consequence, phenotypic expression in prion diseases may be defined in part by the molecular variability of proteolytic processing, which in turn probably is determined by the particular conformation of the different PrP<sup>Sc</sup> isoforms. This does not exclude the role of additional factors in phenotypic expression, in particular, differences in glycosylation that may be especially relevant in the new variant CJD.

The pathology of prion diseases is limited mainly to neural tissues despite the ubiquitous expression of PrP<sup>C</sup>.<sup>3,12</sup> As the factors underlying this restricted distribution are unknown, we also investigated the existence of tissue-specific attributes of PrP<sup>C</sup> and its fragments. Lymphoid tissue (tonsils) and peripheral blood platelets from neurologically normal patients were selected, based on their possible role in the pathogenesis of prion disorders, especially in the peripherally acquired forms.<sup>42,59</sup> Immunoblot analyses showed a proteolysis of PrP<sup>C</sup> analogous but not identical to that in brain. Deglycosylated platelet proteins had a prominent amino-truncated PrP<sup>C</sup> product of 19 kd and minimal amounts of a 16-kd carboxyl-termi-

nal fragment. The 19-kd fragment probably corresponds to the deglycosylated form of a PrP<sup>27-30</sup>-like species released from normal platelets that starts at Gly90.<sup>42</sup> After deglycosylation, tonsil samples contained PrP<sup>C</sup> peptides of 20 to 21 kd detected with antibody 3F4, and an 18-kd peptide signaled only by  $\alpha$ -P214. There also were slight disparities in the molecular weight of the bands corresponding to deglycosylated full-length PrP<sup>C</sup>, possibly due to heterogeneity in the composition of the GPI anchor, differences in PNGase-F accessibility to Asn-linked carbohydrates, limited terminal truncation, or other undefined post-translational modifications. These modifications may affect the position of the lower bands, and thus pattern variability may be due to factors other than the site of cleavage. In addition, the distinct molecular weight of the glycosylated PrP<sup>C</sup> species in platelets and tonsils relative to brain PrP<sup>C</sup> suggests heterogeneity in the composition of the Asn-linked carbohydrates.

Thus, we found several variances in PrP<sup>C</sup> proteolytic cleavage, and probably in the glycosylation and GPI composition of PrP<sup>C</sup>, between neural and non-neural tissues. As PrP<sup>C</sup>-PrP<sup>Sc</sup> interaction appears to be a crucial pathogenic step promoted by homology,<sup>41</sup> the observed differences may modify the rate of prion replication. In agreement with this idea, recent studies have shown that the glycosylation of the PrP<sup>C</sup> isoform in transgenic mice<sup>60</sup> and cell culture systems<sup>61</sup> affects the efficiency of its conversion to the abnormal isoform. Whether this is a mechanism underlying tissue specificity remains an open question. The presence of these differences also is compatible with the hypothesis that replication of peripherally acquired prions first occurs in non-neural tissues, most likely lymphoid organs, where they acquire distinctive molecular features.<sup>23</sup>

### Acknowledgments

We thank the staff and Alice Weiss of the Resource for Tumor Tissues and Data of the Kaplan Cancer Center for providing fresh lymphoid tissues for this study, and Dr. R.J. Kascsak (Institute for Basic Research in Developmental Disabilities) for the monoclonal antibody 3F4.

### References

1. Stahl N, Borchelt DR, Prusiner SB: Differential release of cellular and scrapie prion proteins from cellular membranes by phosphatidylinositol-specific phospholipase. *Biochemistry* 1990, 29:5405-5412
2. Robakis NK, Devine-Gage EA, Jenkins EC, Kascsak RJ, Brown WT, Krawczun MS, Silverman WP: Localization of a human gene homologous to the PrP gene on the p arm of chromosome 20 and detection of PrP-related antigens in normal brain. *Biochem Biophys Res Commun* 1986, 140:758-765
3. Bendheim PE, Brown HR, Rudelli RD, Scala LJ, Goller NL, Wen GY, Kascsak RJ, Cashman NR, Bolton DC: Nearly ubiquitous tissue distribution of the scrapie agent precursor protein. *Neurology* 1992, 42:149-156
4. Kretzschmar HA, Prusiner SB, Stowring LE, DeArmond SJ: Scrapie prion proteins are synthesized in neurons. *Am J Pathol* 1986, 72:1-5
5. Hope J, Morton LDJ, Farquhar CF, Multhaupt G, Beyreuther K, Kimberlin RH: The major polypeptide of scrapie-associated fibrils (SAF) has the same size, charge, distribution and N-terminal protein sequence as predicted for the normal brain protein (PrP). *EMBO J* 1986, 5:2591-2597
6. Mobley WC, Neve RL, Prusiner SB, McKinley MP: Nerve growth factor increases mRNA levels for the prion protein and the beta-amyloid protein precursor in developing hamster brain. *Proc Natl Acad Sci USA* 1988, 85:9811-9815
7. Wion D, Le Bert M, Brachet P: Messenger RNAs of beta-amyloid precursor protein and prion protein are regulated by nerve growth factor in PC12 cells. *Int J Dev Neurosci* 1988, 6:387-393
8. Cashman NR, Loertscher R, Nalbantoglu J, Shaw I, Kascsak RJ, Bolton DC, Bendheim PE: Cellular isoform of the scrapie agent protein participates in lymphocyte activation. *Cell* 1990, 61:185-192
9. Collinge J, Whittington MA, Sidle KC, Smith CJ, Palmer MS, Clarke AR, Jefferys JG: Prion protein is necessary for normal synaptic function. *Nature* 1994, 370:295-297
10. Tobler I, Gaus SE, Deboer T, Achermann P, Fischer M, Rulicke T, Moser M, Oesch B, McBride PA, Manson JC: Altered circadian activity rhythms and sleep in mice devoid of prion protein. *Nature* 1996, 380:639-642
11. Yehiely F, Bamborough P, Da Costa M, Perry BJ, Thinakaran G, Cohen FE, Carlson GA, Prusiner SB: Identification of candidate proteins binding to prion protein. *Neurobiol Dis* 1997, 3:339-355
12. Budka H, Aguzzi A, Brown P, Brucher JM, Bugiani O, Gullotta F, Haltia M, Hauw JJ, Ironside JW, Jellinger K, Kretzschmar HA, Lantos PL, Masullo C, Schlote W, Tateishi J, Weller RO: Neurological diagnostic criteria for Creutzfeldt-Jakob disease (CJD) and other human spongiform encephalopathies (prion diseases). *Brain Pathol* 1995, 5:459-466
13. Prusiner SB: Molecular biology and pathogenesis of prion diseases. *Trends Biochem Sci* 1996, 21:482-487
14. Bolton DC, McKinley MP, Prusiner SB: Identification of a protein that purifies with the scrapie prion. *Science* 1982, 218:1309-1311
15. Oesch B, Westaway D, Wälchli M, McKinley MP, Kent SBH, Aebersold R, Barry RA, Tempst P, Teplow DB, Hood LE, Prusiner SB, Weissman C: A cellular gene encodes scrapie PrP 27-30 protein. *Cell* 1985, 40:735-746
16. Meyer RK, McKinley MP, Bowman KA, Braunfeld MB, Barry RA, Prusiner SB: Separation and properties of cellular and scrapie prion protein. *Proc Natl Acad Sci USA* 1986, 83:2310-2314
17. Borchelt DR, Scott M, Taraboulos A, Stahl N, Prusiner SB: Scrapie and cellular prion protein differ in their kinetics of synthesis and topology in cultured cells. *J Cell Biol* 1990, 110:743-752
18. Pan KM, Baldwin M, Nguyen J, Gasset M, Serban A, Groth D, Mehlhorn I, Huang Z, Fletterick RJ, Cohen FE, Prusiner SB: Conversion of alpha-helices into beta-sheets features in the formation of scrapie prion proteins. *Proc Natl Acad Sci USA* 1993, 90:10962-10966
19. Palmer MS, Dryden AJ, Hughes JT, Collinge J: Homozygous prion protein genotype predisposes to sporadic Creutzfeldt-Jakob disease. *Nature* 1991, 352:340-342
20. Collinge J, Palmer MS, Dryden AJ: Genetic predisposition to iatrogenic Creutzfeldt-Jakob disease. *Lancet* 1991, 337:1441-1442
21. Goldfarb LG, Petersen RB, Tabaton M, Brown P, LeBlanc AC, Montagna P, Cortelli P, Julien J, Vital C, Pendelbury WW, Haltia M, Wills PR, Hauw JJ, McKeever PE, Monari L, Schrank B, Swergold GD, Auttilio-Gambetti L, Gajdusek DC, Lugaresi E, Gambetti P: Fatal familial insomnia and familial Creutzfeldt-Jakob disease: disease phenotype determined by a DNA polymorphism. *Science* 1992, 258:806-808
22. Prusiner SB: Inherited prion diseases. *Proc Natl Acad Sci USA* 1994, 91:4611-4614
23. Collinge J, Sidle KC, Meads J, Ironside J, Hill AF: Molecular analysis of prion strain variation and the aetiology of "new variant" CJD. *Nature* 1996, 383:685-690
24. Telling GC, Scott M, Mastrianni J, Gabizon R, Torchia M, Cohen FE, DeArmond SJ, Prusiner SB: Prion propagation in mice expressing human and chimeric PrP transgenes implicates the interaction of cellular PrP with another protein. *Cell* 1995, 83:79-90
25. Telling GC, Scott M, Hsiao KK, Foster D, Yang SL, Torchia M, Sidle KC, Collinge J, DeArmond SJ, Prusiner SB: Transmission of Creutzfeldt-Jakob disease from humans to transgenic mice expressing chimeric human-mouse prion protein. *Proc Natl Acad Sci USA* 1994, 91:9936-9940
26. Chen SG, Teplow DB, Parchi P, Teller JK, Gambetti P, Auttilio-Gambetti L: Truncated forms of the human prion protein in normal brain and in prion diseases. *J Biol Chem* 1995, 270:19173-19180

27. Gasset M, Baldwin MA, Lloyd DH, Gabriel JM, Holtzman DM, Cohen F, Fletterick R, Prusiner SB: Predicted alpha-helical regions of the prion protein when synthesized as peptides form amyloid. *Proc Natl Acad Sci USA* 1992, 89:10940–10944
28. Huang Z, Prusiner SB, Cohen FE: Scrapie prions: a three-dimensional model of an infectious fragment. *Fold Des* 1996, 1:13–19
29. Peretz D, Williamson RA, Matsunaga Y, Serban H, Pinilla C, Bastidas RB, Rozenshteyn R, James TL, Houghten RA, Cohen FE, Prusiner SB, Burton DR: A conformational transition at the N terminus of the prion protein features in formation of the scrapie isoform. *J Mol Biol* 1997, 273:614–622
30. James TL, Liu H, Ulyanov NB, Farr-Jones S, Zhang H, Donne DG, Kaneko K, Groth D, Mehlhorn I, Prusiner SB, Cohen FE: Solution structure of a 142-residue recombinant prion protein corresponding to the infectious fragment of the scrapie isoform. *Proc Natl Acad Sci USA* 1997, 94:10086–10091
31. Parchi P, Castellani R, Capellari S, Ghetti B, Young K, Chen SG, Farlow M, Dickson DW, Sima AAF, Trojanowski JQ, Petersen RB, Gambetti P: Molecular basis of phenotypic variability in sporadic Creutzfeldt-Jakob disease. *Ann Neurol* 1996, 39:767–778
32. Gearing M, Mirra SS, Hedreen JC, Sumi SM, Hansen LA, Heyman A: The consortium to establish a registry for Alzheimer's disease (CERAD). X. Neuropathology confirmation of the clinical diagnosis of Alzheimer's disease. *Neurology* 1995, 45:461–466
33. Schlossmacher MG, Ostaszewski BL, Hecker LI, Celi A, Haas C, Chin D, Lieberburg I, Furie BC, Selkoe DJ: Detection of distinct isoform patterns of the beta-amyloid precursor protein in human platelets and lymphocytes. *Neurobiol Aging* 1992, 13:421–434
34. Dlouhy SR, Hsiao K, Farlow MR, Forud T, Conneally PM, Johnson P, Prusiner SB, Hodes ME, Ghetti B: Linkage of the Indiana kindred of Gerstmann-Sträussler-Scheinker disease to the prion protein gene. *Nature Genet* 1992, 1:64–67
35. Bolton DC, Seligman SJ, Bablanian G, Windsor D, Scala LJ, Kim KS, Chen CM, Kascak RJ, Bendheim PE: Molecular location of a species-specific epitope on the hamster scrapie agent protein. *J Virology* 1991, 65:3667–3675
36. Xi YG, Cardone F, Pocchiari M: Detection of proteinase-resistant protein (PrP) in small brain tissue samples from Creutzfeldt-Jakob disease patients. *J Neurol Sci* 1994, 124:171–173
37. Fischer M, Rüllicke T, Raeber A, Sailer A, Moser M, Oesch B, Brandner S, Aguzzi A, Weissmann C: Prion protein (PrP) with amino-proximal deletions restoring susceptibility of PrP knockout mice to scrapie. *EMBO J* 1996, 15:1255–1264
38. Haraguchi T, Fisher S, Olofsson S, Endo T, Groth D, Tarantino A, Borchelt DR, Teplow DB, Hood L, Burlingame A, Lycke E, Kobata A, Prusiner SB: Asparagine-linked glycosylation of the scrapie and cellular prion proteins. *Arch Biochem Biophys* 1989, 274:1–13
39. Piccardo P, Seiler C, Dlouhy SR, Young K, Farlow MR, Prelli F, Frangione B, Bugiani O, Tagliavini F, Ghetti B: Proteinase-K resistant prion protein isoforms in Gerstmann-Sträussler-Scheinker disease (Indiana kindred). *J Neuropathol Exp Neurol* 1996, 55:1157–1163
40. Medori R, Tritschler HJ, LeBlanc A, Villare F, Manetto V, Chen HY, Xue R, Leal S, Montagna P, Cortelli P, Tinuper P, Avoni P, Mochi M, Baruzzi A, Hauw JJ, Ott J, Lagaresi E, Autilio-Gambetti L, Gambetti P: Fatal familial insomnia, a prion disease with a mutation at codon 178 of the prion protein gene. *N Engl J Med* 1992, 326:444–449
41. Prusiner SB, Scott M, Foster D, Pan KM, Groth D, Mirenda C, Torchia M, Yang S-L, Serban D, Carlson GA, Hoppe PC, Westaway D, DeArmond S: Transgenic studies implicate interactions between homologous PrP isoforms in scrapie prion replication. *Cell* 1990, 63:673–686
42. Perini F, Vidal R, Ghetti B, Tagliavini F, Frangione B, Prelli F: PrP27–30 is a normal soluble prion protein fragment released by human platelets. *Biochem Biophys Res Commun* 1996, 223:572–577
43. Palmer MS, Collinge J: Mutations and polymorphisms in the prion protein gene. *Hum Mutat* 1993, 2:168–173
44. Wisniewski T, Frangione B: Apolipoprotein E: a pathological chaperone protein in patients with cerebral and systemic amyloid. *Neurosci Lett* 1992, 135:235–238
45. Carlson GA, Ebeling C, Yang S-L, Telling G, Torchia M, Groth D, Westaway D, DeArmond SJ, Prusiner SB: Transmission of Creutzfeldt-Jakob disease from humans to transgenic mice expressing chimeric human-mouse prion protein. *Proc Natl Acad Sci USA* 1994, 91:5690–5694
46. Gasset M, Baldwin MA, Fletterick RJ, Prusiner SB: Perturbation of the secondary structure of the scrapie prion protein under conditions that alter infectivity. *Proc Natl Acad Sci USA* 1993, 90:1–5
47. Heller J, Kolbert AC, Larsen R, Ernst M, Bekker T, Baldwin M, Prusiner SB, Pines A, Wemmer DE: Solid-state NMR studies of the prion protein H1 fragment. *Protein Sci* 1996, 5:1655–1661
48. Hornemann S, Korth C, Oesch B, Riek R, Wider G, Wüthrich K, Glockshuber R: Recombinant full-length murine prion protein, mPrP(23–231): purification and spectroscopic characterization. *FEBS Lett* 1997, 413:277–281
49. Hsiao K, Baker HF, Crow TJ, Poulter M, Owen F, Terwilliger JD, Westaway D, Ott J, Prusiner SB: Linkage of a prion protein missense variant to Gerstmann-Sträussler-Scheinker syndrome. *Nature* 1989, 338:342–345
50. Harris DA, Huber MT, van Dijken P, Shyng SL, Chait BT, Wang R: Processing of a cellular prion protein: identification of N- and C-terminal cleavage sites. *Biochemistry* 1993, 32:1009–1016
51. Singh N, Zanusso G, Chen SG, Fujioka H, Richardson S, Gambetti P, Petersen RB: Prion protein aggregation reverted by low temperature in transfected cells carrying a prion protein gene mutation. *J Biol Chem* 1997, 272:28461–28470
52. Miura T, Hori-i A, Takeuchi H: Metal-dependent alpha-helix formation promoted by the glycine-rich octapeptide region of prion protein. *FEBS Lett* 1996, 396:248–252
53. Guiry DC, Wakayama I, Liberski PP, Gajdusek DC: Relationship of microglia and scrapie amyloid-immunoreactive plaques in kuru, Creutzfeldt-Jakob disease and Gerstmann-Sträussler syndrome. *Acta Neuropathol (Berl)* 1994, 87:526–530
54. Tagliavini F, Prelli F, Ghiso J, Bugiani O, Serban D, Prusiner SB, Farlow MR, Ghetti B, Frangione B: Amyloid protein of Gerstmann-Sträussler-Scheinker disease (Indiana kindred) is an 11 kd fragment of prion protein with an N-terminal glycine at codon 58. *EMBO J* 1991, 10:513–519
55. Tagliavini F, Prelli F, Porro M, Rossi G, Giaccone G, Farlow MR, Dlouhy SR, Ghetti B, Bugiani O, Frangione B: Amyloid fibrils in Gerstmann-Sträussler-Scheinker disease (Indiana and Swedish kindreds) express only PrP peptides encoded by the mutant allele. *Cell* 1994, 79:695–703
56. Forloni G, Del Bo R, Angeretti N, Chiesa R, Monzani E, Salmona M, Bugiani O, Tagliavini F: Neurotoxicity of a prion protein fragment. *Nature* 1993, 362:543–545
57. Tagliavini F, Prelli F, Verga L, Giaccone G, Sarma R, Gorevic P, Ghetti B, Passerini F, Ghibaudi E, Forloni G, Salmona M, Bugiani O, Frangione B: Synthetic peptides homologous to prion protein residues 106–147 form amyloid-like fibrils in vitro. *Proc Natl Acad Sci USA* 1993, 90:9678–9682
58. Castaño EM, Frangione B: Non-Alzheimer's disease amyloidoses of the nervous system. *Curr Opin Neurol* 1995, 8:279–285
59. Eklund CM, Kennedy RC, Hadlow WJ: Pathogenesis of scrapie virus infection in the mouse. *J Infect Dis* 1967, 117:15–22
60. DeArmond SJ, Sanchez H, Yehiely F, Qiu Y, Ninchak-Casey A, Daggett V, Camerino AP, Cayetano J, Rogers M, Groth D, Torchia M, Tremblay P, Scott MR, Cohen FE, Prusiner SB: Selective neuronal targeting in prion disease. *Neuron* 1997, 19:1337–1348
61. Lehmann S, Harris DA: Blockade of glycosylation promotes acquisition of scrapie-like properties by the prion protein in cultured cells. *J Biol Chem* 1997, 272:21479–21487